DJS Vol. 51(1)(2025) – pp.9-22 ISSN: 1012-5965

Delta Journal of Science

Available online at
https://djs.journals.ekb.eg/

Research Article

PHYSICS

Controlling the crystalline nature and optical properties of PVA by adding CS as a modifier

M.A. Ouda*, O.M. Hemeda, A.A. El-Sebaii, M.R.I. Ramadan, Ali Ibrahim

Physics department, Faculty of Science, Tanta University, Egypt

*Corresponding author: M.A. Ouda E-mail: muhammad.alaa@science.tanta.edu.eg

Received: 16/5/2025 **Accepted:** 20/7/2025

KEY WORDS

Polyvinyl alcohol (PVA)
Chitosan (CS)
Polymer blend films
Optical band gap
Dielectric properties
UV–Vis spectroscopy
CdS doping

ABSTRACT

This study uniquely explores the systematic tuning of optical band gaps in PVA/CS polymer blends by varying chitosan concentrations, correlating structural amorphous phase changes with precise optical property modifications. This approach offers new insights for optimizing polymer blends for optoelectronic and solar energy applications.

In this study, polyvinyl alcohol (PVA) and chitosan (CS) polymer blend was prepared using the solvent casting technique. The resulting films were characterized by X-ray diffraction (XRD), ultraviolet–visible (UV–Vis) spectroscopy, and Fourier-transform infrared (FTIR) spectroscopy were utilized to characterize the samples. XRD analysis was specifically used to examine the structural properties and to verify the presence of an amorphous phase. UV-Vis measurements revealed a declining pattern in the optical band gap conjunction with increasing CS content. The direct band gap decreased from 4.77 eV for pure PVA to 4.56 eV, 4.58 eV, and 4.36 eV for CS concentrations of 20%, 50%, and 80%, respectively, and further to 4.02 eV for pure CS. A similar decreasing trend was observed for the indirect band gap, which dropped from 5.27 eV for pure PVA to 4.09 eV for pure CS. These results indicate that the controlled modification of crystallinity and optical band gap via chitosan blending makes the PVA/CS films promising candidates for optoelectronic and solar energy-related applications.

Introduction

Although the structural and optical characteristics of individual PVA and CS films have been widely investigated, studies focusing on the systematic tuning of crystallinity and optical band gap through controlled chitosan incorporation into PVA matrices remain limited. In particular, the direct correlation between CS concentration and the resulting optical band gap and crystalline behavior has not been extensively explored. This study addresses this gap by investigating the effect of different CS ratios on the crystalline structure and band gap behavior of PVA/CS blend films.

Blending polymers is a promising approach to overcome the limitations of individual polymers and to develop new materials with unique properties suitable for a wide range of applications **(Mostafa and Menazea, 2020; Dorigato, 2021).** Moreover, using low-cost polymer blends has been shown to enhance both the chemical and physical properties of the resulting materials. Among these, the natural polysaccharide chitosan (CS) has gained considerable attention due to its low cost and ease of production. CS is recognized as a biopolymer and biomaterial with the ability to form films independently or when blended with other polymers. Owing to its excellent biocompatibility, non-toxicity, biodegradability, antimicrobial activity, and wound healing capabilities, CS has been widely used in biomedical applications, particularly in drug delivery systems **(Meikhail et al., 2018).**

Similarly, polyvinyl alcohol (PVA) is one of the most important synthetic and biodegradable polymers, extensively utilized in various fields **(Abdelrazek et al., 2010; Elashmawi and Menazea, 2019)**, including implants, prosthetic devices, contact lenses, fibers, films, pharmaceuticals, and cosmetics **(Abdelrazek et al., 2010)**. Its significance stems from its water solubility, which depends on its molecular weight and the presence of active hydroxyl groups in its semi-crystalline structure. These functional groups facilitate strong hydrogen bonding, enabling PVA to form films either alone or when blended with other polymers **(Menazea et al., 2020)**.

To improve the properties of polymer blends, fillers, whether organic or inorganic—can be incorporated. However, despite the advantageous characteristics of the PVA/CS hybrid matrix, it still demonstrates limitations in electrical and optical performance. Therefore, reinforcing such matrices with nanomaterials has become a promising strategy for advancing bioelectronic and optoelectronic applications without relying on metallic components. Nonetheless, the structural, optical, and electrical characteristics of the PVA/CS blend still require further enhancement **(Karimi et al., 2009; Najm et al., 2022)**.

In this work, polymer blend films based on PVA and CS were prepared at three different blend ratios. Additionally, pure PVA and pure CS films were fabricated for comparison. All films were analyzed using X-ray diffraction (XRD) to investigate their structural properties, Fourier-transform infrared spectroscopy (FTIR), and UV–visible absorption spectroscopy (UV-Vis) to examine their optical properties. The effect of CS content on the crystallinity and optical band gap was systematically studied. The findings contribute to a better

understanding of the structure–property relationships in polymer blends for potential optoelectronic and solar cells applications.

Experimental Methods

Materials

Chitosan (CH_{266}), with a molecular weight ranging from 300,000 to 350,000 Da, and a degree of deacetylation ≥ 85%, was obtained from Alpha Chemika, Polyvinyl alcohol $(-C_2H_4O)_n$ with a molecular weight of 115,000 g/mol and a degree of hydrolysis of 98–99%, was purchased from Oxford Laboratory Reagent (Neminath, India). All chemicals used were of analytical grade and used without further purification. Glacial acetic acid (98%) and distilled water were used in the preparation of polymer solutions

Preparation of PVA

The PVA film was prepared by dissolving 7.5 g of PVA powder in 125 mL of distilled water under magnetic stirring. The mixture was heated to 90°C, then allowed to cool gradually to 40°C while stirring continued until the powder was completely dissolved and a clear solution was obtained.

Preparation of CS

To prepare 300 mL of CS solution, 3 g of chitosan (CS) powder was dissolved in a solvent mixture consisting of 100 mL of dist. water and 6 mL of acetic acid (98%). The solution was stirred continuously at 25°C for 1 hour until the chitosan was completely dissolved, forming a homogenous, slightly viscous solution.

Preparation of PVA/Chitosan blend

To prepare the PVA/Chitosan (PVA/CS) blend films, appropriate volumes of the previously prepared PVA and CS solutions were mixed in different weight ratios (20:80, 50:50, and 80:20). The blends were magnetically stirred at room temperature for approximately 1 hour to ensure complete homogeneity. After mixing thoroughly, the resulting blend solutions were poured into clean, leveled glass Petri dishes and allowed to dry at room temperature for 3 days. Once fully dried, the films were gently peeled off the Petri dishes and stored in a desiccator for further characterization. The thickness of the prepared films was measured using a digital micrometer (accuracy ±1 µm) at multiple points across each sample to ensure uniformity. The average thickness was found to be in the range of 70–100µm, depending on the composition and drying conditions. All measurements were performed at room temperature after completing film drying. The selected PVA/CS weight ratios of 20:80, 50:50, and 80:20 were chosen based on prior studies reporting significant changes in structural and optical behavior within this range **(Hassan et al., 2002; Xavier 2014)**. These ratios provide a systematic framework to study the effect of increasing CS content on film crystallinity and optical performance. Notably, the 50:50 composition is frequently cited in literature as a balanced blend that offers optimal film-forming ability, good miscibility, and enhanced biocompatibility, making it particularly promising for applications in optoelectronics, sensors, and biomedical fields **(Bartczak and Galeski, 2014; Najm et al., 2022**).

After the preparation of the films, no post-processing treatments such as humidity control or annealing were applied. The films were stored and tested under ambient laboratory conditions to preserve their as-prepared properties.

Characterization Techniques

XRD

The crystalline structures of the thin films were evaluated using a Philips model X-

ray diffractometer ($K\alpha$ radiation of Cu, λ = 1.5406 Å) operated at 40 kV and 30 mA . The diffraction patterns were recorded over a 2θ range of 5–80°. The degree of crystallinity of the samples was determined by deconvoluting the XRD patterns into crystalline and amorphous components and calculating the crystallinity index (X_c) using the equation:

$$X_c = \frac{A_c}{A_t}$$

Where A_c is the area under the crystalline peaks and A_t (total area) is the area under the amorphous background and crystalline peaks. This analysis was carried out using Origin software to fit and integrate the peaks. All measurements and data processing were conducted at the Central Lab, Kafr El-Sheikh University.

FTIR

Infrared spectra of the prepared samples were recorded at ambient temperature using a PerkinElmer 1430 FTIR spectrometer at the Central Laboratory, Tanta University. Measurements were carried out in transmission mode, in the spectral range of 400–4000 cm^{-1}, with a spectral resolution of 4 cm^{-1} and averaging 16 scans per sample. All films were analyzed in dry form after complete solvent evaporation.

UV-Vis

The optical properties for the samples are investigated by using Ultraviolet–Visible spectrometer (SHIMADZU, UV-2600i) in the range of 190–700 nm with fixed step of 1 nm. (Electronics Lab, Faculty of Science, Tanta, University).

Results and Discussion

XRD Analysis

The structural characteristics of the polymer matrix doped with varying concentrations of chitosan (CS) were examined using X-ray diffraction (XRD). The pattern of pure PVA has two obvious peaks. The first one at 2θ ≈ 19.7° which is corresponding to (101) plane of PVA crystal structure. This peak is an indicator for the semi-crystalline nature of PVA which is attributed to the intense intermolecular hydrogen bonds that exist between adjacent PVA chains **(Liu et al., 2019a).** The second peak which is at 2θ ≈ 43.9° indexed to (100), is evidence for the amorphas phase for PVA **(Cui et al., 2006)**.

The intensity of the peaks decreased upon adding CS especially for the second peak which nearly disappeared in all concentrations of CS but the characteristic peak of PVA at 2θ ≈ 19.5° remained prominent in the blends, but its intensity decreased with increasing CS content this is a result for interaction between PVA and CS which can effect on the crystallinity of the PVA matrix **(Prihatiningtyas et al., 2021)**.

The patterns for PVA/CS didn't show any peaks corresponding to Pure CS, indicating that CS is totally dispersed in PVA matrix and integrated in PVA chains **(Han et al., 2021)**.

From Hermans-Weidinger method we can calculate crystallinity fraction (X_c) of thin films **(Bouman and Wijzenbeek, 1966)**:

$$X_c = \frac{A_c}{A_t}$$

Where,

- A_c crystalline peaks' area.
- A_t total peaks' area.

The results showed that the degree of crystallinity of composite thin films

decreased from around 81.8% for Pure PVA to 33.2% as the CS content increased, as illustrated in **Table (1)**. This reduction in crystallinity implies that the addition of CS causes interactions between the CS nanoparticles and the PVA matrix, leading to increasing the amorphous of the samples.

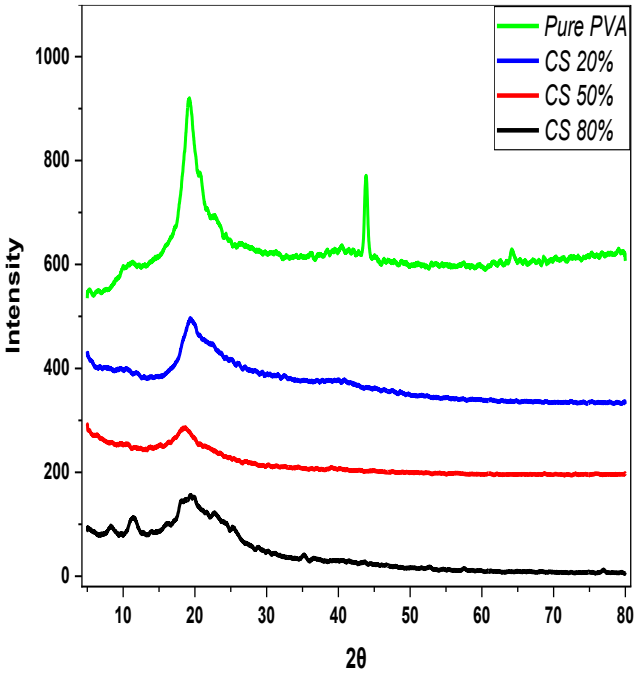

Fig. (1): XRD patterns for Pure PVA and PVA/CS with different concentration ratios.

Table (1): Degree of crystallinity for pure PVA and PVA/CS nanocomposite films.

	Pure PVA	PVA 80	PVA 50	PVA 20
A_c	949.8	492.5	144	193.3
A_t	1161	817.7	297.1	582
X_c	81.8%	60.2%	48.4%	33.2%

FTIR Analysis

The provided FTIR graph shows the transmittance spectrum for different compositions of PVA (Polyvinyl Alcohol) and pure PVA. The "Pure PVA" curve represents the IR spectrum, exhibits the most pronounced peaks corresponding to the characteristic functional groups of the PVA polymer. The first broad peak which is around 3300:3500 cm^{-1} is an indication for water molecule vibration in the PVA polymer **(Qureshi et al., 2021; Jamasri et al., 2023)**. The peaks around 2900 cm^{-1} are assigned to the C-H stretching vibrations from the alkyl group **(Karimi et al., 2009)**. The peak at 1630 cm^{-1} is associated with the C=O stretching vibration which indicates the presence of amide II and amide I **(Ali, 2019)**. The vibrational signal of the methylene groups corresponding to the bending of the -OH groups was recorded at around 1460 cm^{-1}, while the signal corresponding to C-O stretching was noted at 1092 cm^{-1}. The lower wavenumber peaks, such as around 860-880 cm^{-1}, are related to the C-C and C-O-H bending vibrations. So, it's obvious that the wavelength is shifted to lower wave numbers by increasing chitosan concentrations also the sharpness of the peaks is increased while its broadness decreased. Also, the shift of absorption band frequency low values indicating that adding CS influences PVA polymer chain and acts as a modifier.

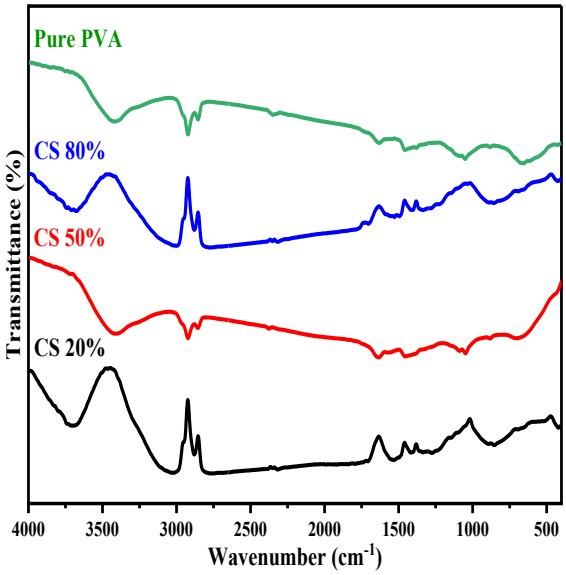

Fig. (2): FTIR spectra of PVA and PVA/CS blends.

Table (2): Characteristic FTIR absorption bands observed in pure PVA and PVA/CS blends.

Wavenumber (cm^{-1})		Vibrational Modes
Pure PVA	**PVA/CS**	
3453	3438	O-H stretching
2981	2929	C-H stretching
1633	1633	C=O stretching
1485	1457	C-H bending
1092	1024	C-O stretching
686	861	C-C and C-O-H bending

UV/Vis Analysis

Absorption and Absorption coefficient

Fig. (3) shows the UV-Vis absorption spectrum of Pure PVA has a characteristic peak in UV-region at around 200 nm due to electronic transitions π-π* of the vinyl alcohol groups. Upon adding CS, the transition peaks sharpness decreased and slightly shifted towards higher wavelengths due to the crystallinity nature of PVA and amorphous nature of CS. The CS acts as a modifier to PVA matrix, its intensity and broadening increases by increasing CS content. This suggests that the presence of CS affects the electronic transitions in PVA. These changes can be linked to new electronic states due to the interaction between PVA and CS **(Liu et al., 2019b)**. From the **Fig. (4)** we can deduce that adding CS increases the absorption coefficient which means that the material's ability to absorb light at a specific wavelength is increased. The second peak for Pure PVA line which is around 280nm may be associated with π-π* transitions of residual carbonyl or conjugated structures that may have been introduced during the PVA synthesis process or as impurities

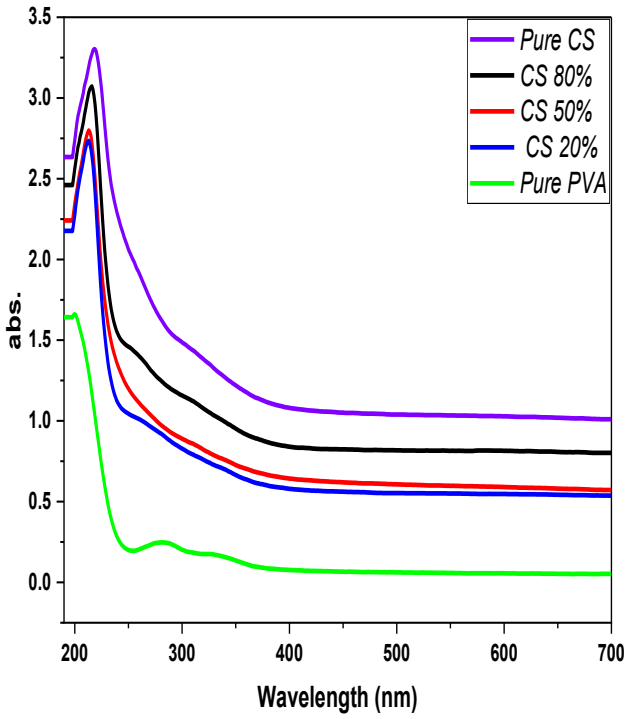

Fig. (3): UV-Vis absorption spectra for Pure PVA, Pure CS and PVA/CS blends with different weight ratios (80/20, 50/50, and 20/80).

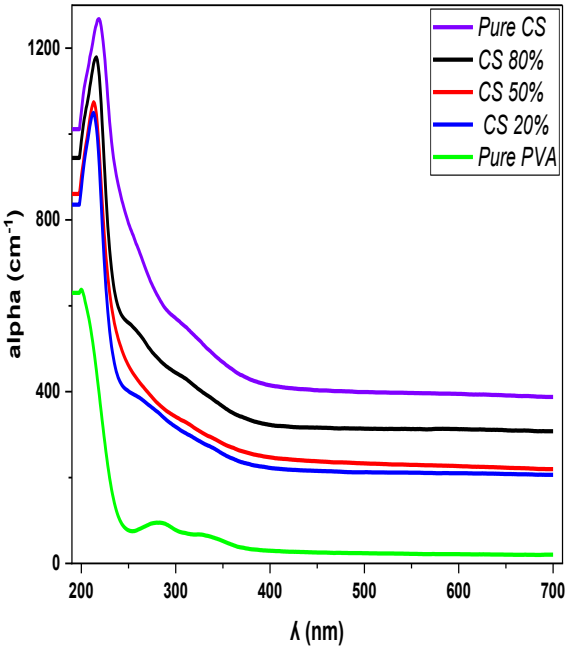

Fig. (4): UV-Vis absorption coefficient spectra for Pure PVA, Pure CS and PVA/CS polymer blends.

Refractive index

The provided graph **Fig. (5)** illustrates the refractive index (n) as a function of wavelength (190–700 nm) for Pure PVA, Pure CS and their blends (PVA/CS) at different ratios (80/20, 50/50, 20/80).

For Pure PVA, the refractive index (n) decreases by increasing the wavelength which is typical for dielectric materials. Also (n) increases with increases the CS concentration. Adding CS introduced a strong interaction with PVA matrix, through hydrogen bonding, which results in a more compact structure, which will in turn play an important role in improving molecular alignment then increasing the material's optical density and polarizability, which directly raises the refractive index **(Singh and Kumar, 2019)**. The refractive index becomes stable as the wavelength tends towards visible regions **(Haider et al., 2020)**. This increase in refractive index of films by adding CS makes these materials suitable for applications requiring tailored optical properties, such as in sensors, optical devices, and coatings **(Farea et al., 2021)**. The result reveals that the refractive index has a direct relationship with absorption coefficient, and both are increased with increasing CS content.

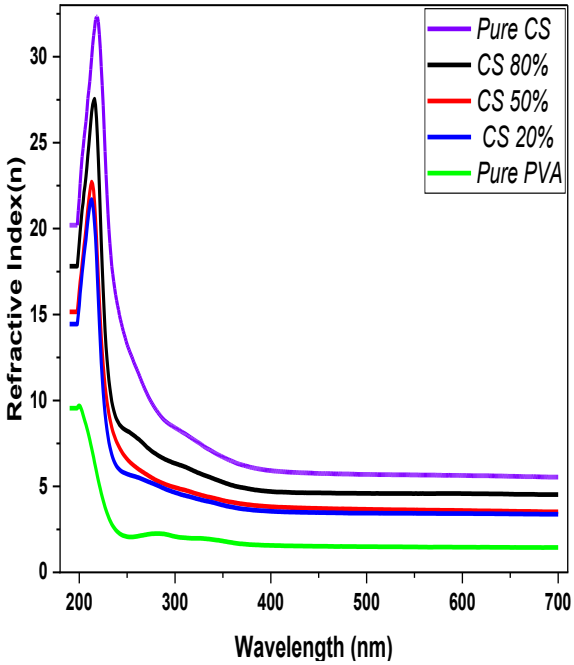

Fig. (5): Refractive index vs. wavelength for pure PVA, pure CS and PVA/CS films.

Band Gap

The optical energy band gap of PVA/CS with three different concentrations was analyzed using Tauc plot equation **(Yasmeen et al., 2019; Alharthi and Badawi, 2023)**

$$(\alpha h\nu)^n = A(h\nu - E_g)$$

Where, α: Absorption coefficient (cm^{-1}), $h\nu$: Photon energy (eV), E_g: Optical energy gap (eV).

A: Proportionality constant related to the material and UV device. n: Depends upon the type of electronic transition:

- n= 1/2: Refers to direct allowed transitions. Fig. (6)

- n= 2: Refers to indirect allowed transitions. Fig. (7)

The fitting of the Tauc plots was performed by selecting the linear portion of the $(\alpha h\nu)^n$ versus $h\nu$ curve, where n = 1/2 for direct allowed transitions and n=2 for indirect allowed transitions. The selection of the fitting range was carefully done to include only the linear region near the absorption edge, avoiding regions affected by noise or excitonic effects. This range selection is critical because fitting outside the linear region can lead to inaccurate estimation of the optical band gap. For each film composition, the linear region was identified visually by plotting the data and fitting the straight-line segment. The extrapolation of this linear fit to the energy axis intercept gives the band gap energy E_g Variation in the fitting range can cause slight deviations in the calculated E_g values, so consistency was maintained by using the same energy range criteria across all samples for comparative analysis.

The calculated values of direct band gap are listed on **Table (3)**. This behavior can be explained by the disruption of crystallinity of PVA by adding CS, which is more amorphous, while increasing the disorder in the blend. Increased amorphous content reduces the shift in the band gap caused by the formation of new localized states in the material.

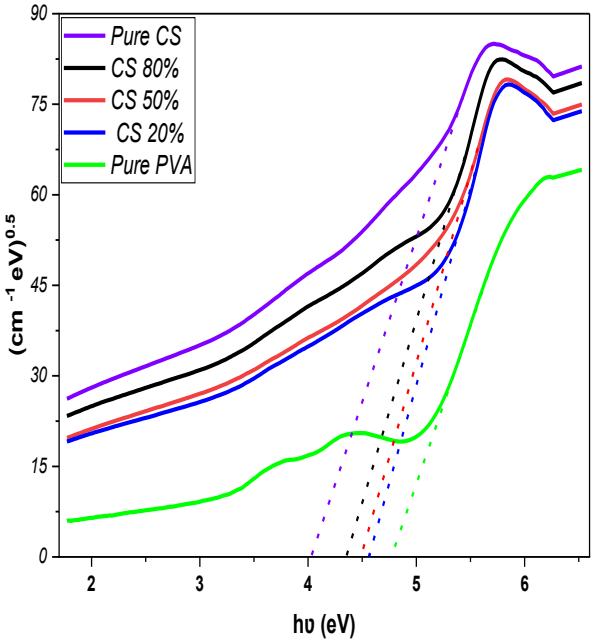

Fig. (6): Tauc's plots of direct status of PVA/CS films.

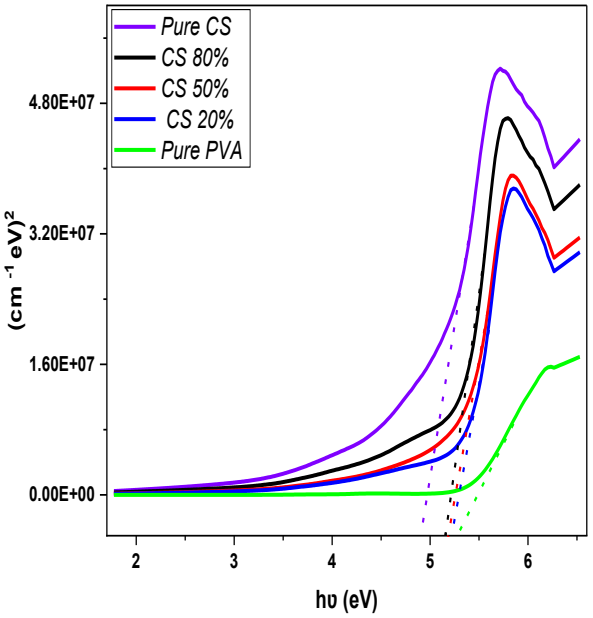

Fig. (7): Tauc's plots of indirect status of PVA/CS films.

Table (3): Direct and indirect B.G values for the samples.

Sample	Direct B.G n=0.5	In-Direct B.G n=2
Pure PVA	4.77	5.27
CS 20%	4.56	5.22
CS 50%	4.48	5.18
CS 80%	4.36	5.14
Pure CS	4.02	4.09

Extinction coefficient (K)

The extinction coefficient represents how much light absorbed and scattered inside the material.

$$A = Kcl$$

Where, A is the absorbance, K is the extinction coefficient, c is the concentration of the species responsible for absorption (mol/L) and l is the path length (cm).

Fig. (8) illustrates the relationship between the extinction coefficient (k) and wavelength for Pure PVA, CS20%, CS50%, CS80% and Pure CS samples. As the concentration of chitosan (CS) increases, the extinction coefficient increases, indicating changes in light absorption properties. This increase is due to the presence of amino and hydroxyl groups in chitosan, which interact with PVA via hydrogen bonding, enhancing absorption in the UV and visible regions **(Mariconda et al., 2019)**. For the lowest CS content (CS20%), the extinction coefficient is at its lowest value because of the semi-crystalline nature of PVA, which limits the extent of absorptive interactions. As the CS concentration increases to 50:50, the extinction coefficient rises due to significant disruption of PVA's crystallinity and increased interactions between the PVA matrix and chitosan **(Hassan et al., 2018)**. For the highest concentration of CS (CS80%), the material becomes mostly amorphous, leading to strong absorption in the UV region **(Kwon et al., 2017)**. The decrease in the extinction coefficient after the initial peak in the UV region occurs due to the reduction in the electronic transitions such as π-π* or n-π*. However, the subsequent increase after ~360nm can be attributed to the emergence of localized states within the energy gap (cause by impurities, defects or the interaction between PVA and CS), structural changes due to the blending, and light scattering effects within the material. These factors contribute to additional light absorption at longer wavelengths **(El-Tantawy et al., 2004; Hamood et al., 2023).**

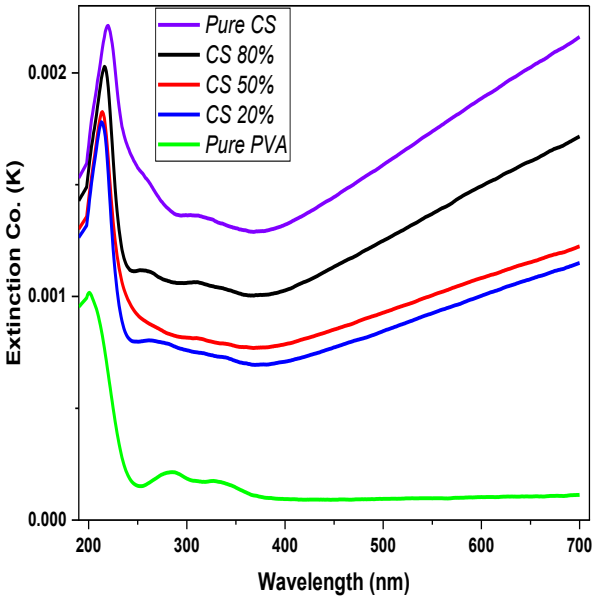

Fig. (8): Extinction Co. vs. wavelength for pure PVA, pure CS and PVA/CS films.

Urbach Energy

Urbach Energy refers to a parameter that characterizes the extent of the exponential tail in the absorption spectrum of the material **(Elashmawi et al., 2023)**. Urbach energy can be calculated from the following equation:

$$\alpha(h\nu) = \alpha_0 \exp\left(\frac{h\nu - E_t}{E_u}\right)$$

Where: $h\nu$ is Photon energy, E_t is Bandgap energy threshold, E_u is Urbach energy and α_0 is a material property constant **(El-Aassar et al., 2023; Elashmawi et al., 2023)**. After plotting $\ln(\alpha)$ verses $h\nu$, we can get E_u from

the reciprocal of the slope of the lines as shown in **Fig. (9)**, the results are listed on the Table (4).

Table (4) shows the variation in E_u with increasing CS content. For pure PVA the $E_u = 0.41\ eV$, this value increased by increasing the concertation of CS to 0.58, 0.69, 0.71 and 1.02 eV **(Darwish *et al.*, 2022)**. By increasing CS content, E_u is increased which indicates that material disorder increasing results are confirmed by XRD analysis of the blend polymer (PVA/CS) increased which indicates that material disorder increasing results are confirmed by XRD analysis of the blend polymer (PVA/CS).

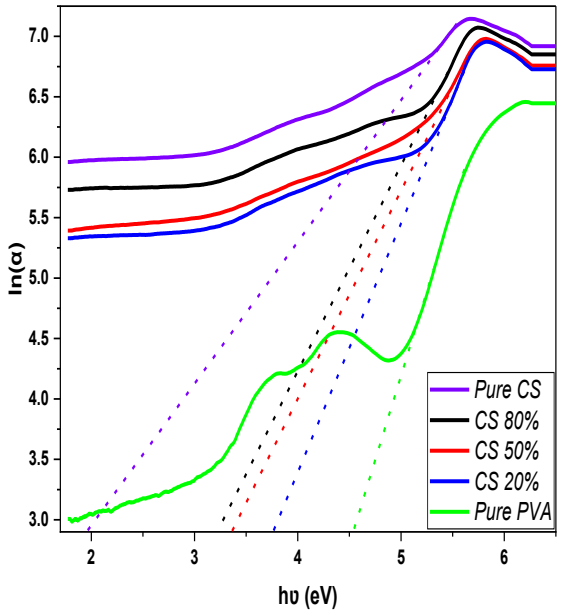

Fig. (9): The plot shows the variation of the natural logarithm of the absorption coefficient (ln(α)) versus photon energy (hv) for samples.

Table (4): Urbach energy values for samples.

Sample	Urbach Energy
Pure PVA	0.41
CS 20%	0.58
CS 50%	0.69
CS 80%	0.70
Pure CS	1.02

Conclusion

The structural and optical analysis of the prepared PVA/Chitosan (CS) blend films reveal a clear correlation between the blend composition, materials' crystallinity and optical properties. XRD results indicate a significant decrease in crystallinity with increasing chitosan content: from 81.81% for pure PVA to 60.23%, 48.47%, and 33.21% for PVA: CS blends of 80:20, 50:50, and 20:80, respectively. This reduction in crystallinity is attributed to the disruption of the semi-crystalline structure of PVA by the amorphous nature of CS, leading to a more disordered arrangement in the polymer matrix.

In parallel, UV-Vis spectroscopy confirms a noticeable decline in direct and indirect optical band gaps with increased CS content. The direct band gap decreased from 4.77 eV for pure PVA to 4.56 eV, 4.48 eV, and 4.36 eV for CS contents of 20%, 50%, and 80%, respectively, reaching 4.02 eV for pure CS. Similarly, the indirect band gap values dropped from 5.27 eV (pure PVA) to 5.22 eV, 5.18 eV, 5.14 eV, and 4.09 eV (pure CS). This reduction in bandgap energies suggests enhanced optical absorption in the visible region, which is desirable for opto-electronic and solar energy applications.

The findings of this study demonstrate that doping PVA/CS films with CdS significantly alters their optical and dielectric properties by reducing the band gap and increasing disorder in the polymer matrix. These modifications suggest potential applications in optoelectronic devices such as photodetectors, solar cells, and sensors, where tunable optical properties are critical.

Furthermore, enhanced dielectric properties indicate suitability for use in capacitive components and flexible electronics.

For future studies, it is recommended to explore the electrical conductivity and charge transport mechanisms in these doped films using techniques like Hall effect measurements and impedance spectroscopy. Additionally, investigating the stability and performance of these films under different environmental conditions could provide valuable insights for practical device fabrication.

References:

Abdelrazek, E. M.; Elashmawi, I. S.; Labeeb, S. (2010). Chitosan filler effects on the experimental characterization, spectroscopic investigation and thermal studies of PVA/PVP blend films, *Physica B*, 405(8): 2021–2027. https://doi.org/10.1016/J.PHYSB.2010.01.095

Alharthi, S. S.; Badawi, A. (2023). Modification of the Structure and Linear/Nonlinear Optical Characteristics of PVA/Chitosan Blend through CuO Doping for Eco-Friendly Applications, *Polymers*, 15(10): 2391. https://doi.org/10.3390/POLYM15102391.

Ali, F. M. (2019). Structural and optical characterization of [(PVA:PVP)-Cu^{2+}] composite films for promising semiconducting polymer devices, *J. Mol. Struct.*, 1189: 352–359. https://doi.org/10.1016/J.MOLSTRUC.2019.04.014.

Bartczak, Z.; Galeski, A. (2014). Mechanical properties of polymer blends, in *Polymer Blends Handbook*, 1203–1297. https://doi.org/10.1007/978-94-007-6064-6_13.

Bouman, J.; Wijzenbeek, M. (1966). Simple Construction for Measuring Internal Friction in Torsion, *Rev. Sci. Instrum.*, 37(10): 1410–1411. https://doi.org/10.1063/1.1720000.

Cui, H. N.; Costa M. F.; Teixeira V.; Zhang J. (2006). Solution-grown method of CdS film by ultrasonical colloid chemistry deposition technique, *Int. J. Photoenergy*, 2006(1): 024916. https://doi.org/10.1155/IJP/2006/24916.

Darwish, M. A.; Zubar T. I.; Kanafyev O. D.; Zhou D.; Trukhanova E. L.; Trukhanov S. V.; Trukhanov A. V.; Henaish A. M. (2022). Combined Effect of Microstructure, Surface Energy, and Adhesion Force on the Friction of PVA/Ferrite Spinel Nanocomposites, *Nanomaterials*, 12(12):1998. https://doi.org/10.3390/NANO12121998.

Dorigato, A. (2021). Recycling of polymer blends, *Advanced Industrial and Engineering Polymer Research*, 4(2): 53–69. https://doi.org/10.1016/J.AIEPR.2021.02.005.

El-Aassar, M. R.; Sendi R. K.; Atta A.; Al-Harbi N.; Rabia M.; Abdelhamied M. M. (2023). Characterization and linear/nonlinear optical properties of PVA/CS/TiO_2 polymer nanocomposite films for optoelectronics applications, *Opt. Quantum Electron.*, 55(14): 1–17. https://doi.org/10.1007/S11082-023-05542-W.

Elashmawi, I. S.; Ismail, A. M.; Abdelghany, A. M. (2023). The incorporation of polypyrrole (PPy) in

CS/PVA composite films to enhance the structural, optical, and electrical conductivity, *Polymer Bulletin*, 80(10): 11379–11399. https://doi.org/10.1007/S00289-022-04611-6.

Elashmawi, I. S.; Menazea, A. A. (2019). Different time's Nd:YAG laser-irradiated PVA/Ag nanocomposites: structural, optical, and electrical characterization, *J. Mater. Res. Technol.*, 8(2): 1944–1951. https://doi.org/10.1016/J.JMRT.2019.01.011.

El-Tantawy F.; Abdel-Kader K.M.; Kaneko F.; Sung. Y.K. (2004). Physical properties of CdS-poly(vinyl alcohol) nanoconducting composite synthesized by organosol techniques and novel application potential", *Eur. Polym. J.*, 40(2): 415–430. https://doi.org/10.1016/J.EURPOLYMJ.2003.10.013.

Farea, M. A.; Mohammed H. Y.; Shirsat S.M.; Sayyad P.W.; Ingle N. N.; Al-Gahouari, M.M.; Mahadik T.; Bodkhe G. A. (2021). Hazardous gases sensors based on conducting polymer composites: Review, *Chem. Phys. Lett.*, 776: 138703. https://doi.org/10.1016/J.CPLETT.2021.138703.

Jamasri J.; Ferriawan Y.; Venditias Y.; Edi S. (2023). Mechanical, Physical and Thermal Characterization of PVA (Polyvinyl Alcohol)/Chitosan Bioplastic Film, *Int. J. Heat Technol.*, 41(3): 687–693. https://doi.org/10.18280/ijht.410322.

Jin-Beom K.; Hyun-Min J.; Hyurk-Choon K.; Sang-Won L. ; Jae-Sung L.; Sae-Wan K.; Ok-Sik K.; Dae-Hyuk K. and Shin-Won K. (2017). Low concentration, multi taste detectable taste sensor using the high transconductance of a cascoded gated lateral bipolar junction transistor, *Sensors and Actuators B: Chemical*, 248: 917–923. https://doi.org/10.1016/J.SNB.2017.01.138.

Hamood F. J.; Yehia M. B.; Kadim Ashraq Mohammed; Abass Kh. H.; Kumar A. M.; Kahtan M. (2023). Effect of CdS Nanoparticles on Structural, Optical and Dielectric Properties for Gamma-Ray Shielding and Antibacterial Efficiency of PVA/PAAm Polymers Blend, *Int. J. Nanotechnol. Appl.*, 22(5). https://doi.org/10.1142/S0219581X23500436.

Haider J.; A.; Al-Shibaany; Z.; Hawy, R.; Hamed, N. (2020). Impact of PS/PMMA Polymer Ratios with Nanocomposite Material on Optical and Morphological Properties, *Ziggurat J. Mater. Technol.*, 1(1): 23–32. https://doi.org/10.36533/ZJMT.V1I1.39

Han H. C.; Gong X. L.; Zhou M.; Li C.; Yang H. B. (2021). A study about silane modification and interfacial ultraviolet aging of hemp fiber reinforced polypropylene composites, *Polymer Composites*, 42(5):2544–2555. https://doi.org/10.1002/PC.26000.

Hassan C. M.; Trakampan P.; Peppas N. A. (2002). Water Solubility Characteristics of Poly(vinyl alcohol) and Gels Prepared by Freezing/Thawing Processes, in *Water Soluble Polymers*, pp. 31–40. https://doi.org/10.1007/0-306-46915-4_3.

Hassan R. U.; Jo S.; Seok J. (2018). Fabrication of a functionally graded and magnetically responsive shape memory polymer using a 3D printing technique

and its characterization, *J. Appl. Polym. Sci.*, 135(11): 45997. https://doi.org/10.1002/APP.45997.

Meysam K.; Mohammad R.; Fathollah M.; Mohammadreza T.; Masoud B. (2009) "RETRACTED: Controlled synthesis, characterization and optical properties of CdS nanocrystalline thin films via chemical bath deposition (CBD) route", *Curr. Appl. Phys.*, 9(6): 1263–1268. https://doi.org/10.1016/J.CAP.2009.02.006.

Meng L.; Lu Y.; Laibing W.; Tengfei M.; Xiaoxiao C.; Yong W.; Wei Z.; Xiulin Z. (2019). Synthesis of monodisperse aromatic azo oligomers toward gaining new insight into the isomerization of π-conjugated azo systems, *Polymer Chemistry*, 10(14): 1806–1811. https://doi.org/10.1039/C9PY00001A.

Mariconda A.; Agovino A.; Sirignano M.; Guadagno L. (2019). Strong Interaction with Carbon Filler of Polymers Obtained by Pyrene Functionalized Hoveyda-Grubbs 2nd Generation Catalyst, *Polymers*, 11(8): 1261. https://doi.org/10.3390/POLYM11081261.

Meikhail; M. S.; Abdelghany A. M. and Awad W. M. (2018). Role of CdSe quantum dots in the structure and antibacterial activity of chitosan/poly-ε-caprolactone thin films, *Egypt. J. Basic Appl. Sci.*, 5(2): 138–144. https://doi.org/10.1016/J.EJBAS.2018.05.003.

Menazea A.A.; Ismail A.M.; Awwad Nasser S. and Ibrahium Hala A. (2020). Physical characterization and antibacterial activity of PVA/Chitosan matrix doped by selenium nanoparticles prepared via one-pot laser ablation route. *J. Mater. Res. Technol.*, 9(5): 9598–9606. https://doi.org/10.1016/J.JMRT.2020.06.077.

Mostafa A. M. and Menazea A.A. (2020). Polyvinyl Alcohol/Silver nanoparticles film prepared via pulsed laser ablation: An eco-friendly nano-catalyst for 4-nitrophenol degradation", *J. Mol. Struct.*, 1212: 128125. https://doi.org/10.1016/J.MOLSTRUC.2020.128125.

Najm A. S.; Naeem H. S.; Majdi H. Sh.; Aishah H. S.; Ali H. H.; Sopian K.; Bais B.; Al-Iessa H. J.; Dhahad H. A.; Ali J. M. and Sultan A. J. (2022). An in-depth analysis of nucleation and growth mechanism of CdS thin film synthesized by chemical bath deposition (CBD) technique, *Scientific Reports*, 12(1): 1–20. https://doi.org/10.1038/S41598-022-19340-Z.

Prihatiningtyas I.,; Hartanto Y.; Ballesteros M.; Sandra R.; Bruggen B. V. (2021) Cellulose triacetate/LUDOX-SiO_2 nanocomposite for synthesis of pervaporation desalination membranes, *J. Appl. Polym. Sci.*, 138(11). https://doi.org/10.1002/APP.50000.

Qureshi D.; Sahoo A.; Mohanty B.; Anis A.; Kulikouskaya V.; Hileuskaya K.; Agabekov V.; Sarkar P.; Ray S. S.; Maji S.; Pal K. (2021). Fabrication and characterization of poly (Vinyl alcohol) and chitosan oligosaccharide-based blend films, *Gels*, 7(2). https://doi.org/10.3390/gels7020055.

Sadaf Y.; Faisal I.; Tauseef M.; Asif N. M.; Asghar M.; Hussain A. (2019). Synthesis, structural and optical

analysis of surfactant assisted ZnO–NiO nanocomposites prepared by homogeneous precipitation method, *Ceramics International*, 45(14): 17859–17873. https://doi.org/10.1016/J.CERAMINT.2019.06.001.

Singh V. and Kumar T. (2019). Study of modified PEDOT:PSS for tuning the optical properties of its conductive thin films, *J. Sci.: Adv. Mater. Devices*, 4(4): 538–543. https://doi.org/10.1016/J.JSAMD.2019.08.009.

Xavier S. F. (2014). Properties and performance of polymer blends, in *Polymer Blends Handbook*, pp. 1031–1201. https://doi.org/10.1007/978-94-007-6064-6_12.

.

التحكم في الطبيعة البلورية والخصائص البصرية لـ PVA بإضافة الكيتوزان كمُعدِّل

محمد علاء عودة*، أسامة محمد حميدة، أحمد السباعي، رأفت رمضان، علي إبراهيم

قسم الفيزياء، كلية العلوم، جامعة طنطا، مصر

تتناول هذه الدراسة بشكل فريد إمكانية الضبط المنهجي للفجوة البصرية في أغشية البوليمرات PVA/CS عن طريق تغيير تراكيز الكيتوزان، وذلك بربط التغيرات في الطور غير المتبلور (الأمورفي) بالتعديلات الدقيقة في الخصائص البصرية. يُقدِّم هذا النهج رؤى جديدة لتحسين خصائص خلطات البوليمرات لاستخدامها في تطبيقات البصريات والإلكترونيات الضوئية والطاقة الشمسية.

تم في هذه الدراسة تحضير خليط بوليمري من كحول البولي فينيل (PVA) والكيتوزان (CS) باستخدام تقنية الصب بالمذيب. تم توصيف الأغشية الناتجة باستخدام تقنيات حيود الأشعة السينية(XRD) ، والمطيافية فوق البنفسجية – المرئية (UV–Vis) ، ومطيافية الأشعة تحت الحمراء بتحويل فورييه .(FTIR) تم استخدام تحليل XRD بشكل خاص لدراسة الخواص التركيبية والتحقق من وجود الطور غير المتبلور.

أظهرت قياسات UV–Vis نمطًا متناقصًا في فجوة الطاقة البصرية المباشرة مع زيادة محتوى الكيتوزان؛ حيث انخفضت الفجوة المباشرة من ٤,٧٧ إلكترون فولت في PVA النقي إلى ٤,٥٦ إلكترون فولت، ٤,٥٨ إلكترون فولت، و٤,٣٦ إلكترون فولت عند تراكيز كيتوزان بنسبة ٢٠٪، ٥٠٪، و٨٠٪ على التوالي، وبلغت ٤,٠٢ إلكترون فولت في CS النقي. كما لوحظ اتجاه مشابه في الفجوة غير المباشرة، حيث انخفضت من ٥,٢٧ إلكترون فولت في PVA النقي إلى ٤,٠٩ إلكترون فولت في CS النقي.

تشير هذه النتائج إلى أن التعديل المنضبط للطبيعة البلورية وفجوة الطاقة البصرية من خلال خلط الكيتوزان يجعل من أغشية PVA/CS مرشحة واعدة لتطبيقات الإلكترونيات الضوئية والطاقة الشمسية.